ORIGINAL ARTICLE

Sergey Kurdyukov · Andrea Faust · Sandra Trenkamp
Sascha Bär · Rochus Franke · Nadia Efremova
Klaus Tietjen · Lukas Schreiber · Heinz Saedler
Alexander Yephremov

Genetic and biochemical evidence for involvement of *HOTHEAD* in the biosynthesis of long-chain α-,ω-dicarboxylic fatty acids and formation of extracellular matrix

Abstract In plants, extracellular matrix polymers built from polysaccharides and cuticular lipids have structural and protective functions. The cuticle is found to be ten times thinner in *Arabidopsis thaliana* (L.) Heynh than in many other plants, and there is evidence that it is unusual in having a high content of α-,ω-dicarboxylic fatty acids (FAs) in its polyesters. We designated the new organ fusion mutant *hth-12* after it appeared to be allelic to *adhesion of calyx edges* (*ace*) and *hothead* (*hth*), upon molecular cloning of the gene by transposon tagging. This mutant is deficient in its ability to oxidize long-chain ω-hydroxy FAs to ω-oxo FAs, which results in leaf polyesters in decreased α-,ω-dicarboxylic FAs and increased ω-hydroxy FAs. These chemical phenotypes lead to disorder of the cuticle membrane structure in *hth-12*. ACE/HTH is a single-domain protein showing sequence similarity to long-chain FA ω-alcohol dehydrogenases from *Candida* species, and we hypothesize that it may catalyze the next step after cytochrome P450 FA ω-hydroxylases in the ω-oxidation pathway. We show that *ACE/HTH* is specifically expressed in epidermal cells. It appears very likely therefore that the changes in the amount of α-,ω-dicarboxylic FAs in *hth-12* reflect the different composition of cuticular polyesters. The *ACE/HTH* gene is also expressed in root epidermal cells which do not form a polyester membrane on the exterior surface, thereby making it possible that the end products of the pathway, α-,ω-dicarboxylic FAs, are generally required for the cross-linking that ensures the integrity of the outer epidermal cell wall.

Keywords *Arabidopsis* · Cuticle · Cutin · Dicarboxylic fatty acids · Epidermis · Extracellular matrix

Abbreviations GC–MS: Gas chromatography–mass spectrometry · RT-PCR: Reverse transcription-polymerase chain reaction · SEM: Scanning electron microscopy · TEM: Transmission electron microscopy · WT: Wild type

S. Kurdyukov · A. Faust · S. Bär · N. Efremova · H. Saedler
A. Yephremov (✉)
Max-Planck-Institut für Züchtungsforschung,
Carl von Linné Weg 10, 50829 Cologne, Germany
E-mail: efremov@mpiz-koeln.mpg.de
Fax: +49-221-5062113

S. Trenkamp · K. Tietjen
Bayer AG, Bayer CropScience, Research, Target Research,
Building 6240, 40789 Monheim, Germany

R. Franke · L. Schreiber
Institut für Zelluläre und Molekulare Botanik, Universität Bonn,
Kirschallee 1, 53115 Bonn, Germany

Present address: S. Kurdyukov
ARC Centre of Excellence for Integrative Legume Research,
School of Environmental and Life Sciences,
University of Newcastle, University Drive,
2308 Callaghan, NSW, Australia

Introduction

The cuticle deposited on the epidermal cell wall is one of the most important adaptations for the terrestrial life of land plants. The structure and chemical composition of the plant cuticle have been intensively studied (Kolattukudy 2001b; Nawrath 2002). The cuticle proper formed beneath the outermost layer, epicuticular wax, often has a lamellate appearance and is seen as darkly staining material in electron micrographs. Whereas the cuticle proper is a lipid-based polymeric coating free of cellulose, with cutin as its major component, the inner layer of the cuticle is formed from an outer portion of the epidermal cell wall. This cuticular layer of the cell wall is impregnated with lipid polymers. Cutin is polyester that can be hydrolyzed in many plants studied to date into a mixture of C16 and C18 hydroxy and epoxy fatty acids (FAs) and glycerol (Kolattukudy 2001a; Nawrath 2002). However, recent work in our lab and by others (Bonaventure et al. 2004; Yephremov et al. 2004;

Franke et al. 2005) has identified α-,ω-dicarboxylic FAs as major cuticular monomers in *Arabidopsis*.

Among the dozens of molecularly cloned genes that, so far, have been shown to play a role in the formation of cuticle in *Arabidopsis* (Yephremov and Schreiber 2005), *FDH*, *LCR*, *WAX2/YRE*, *LACS2*, *ACC1*, and *ATT1* (Yephremov et al. 1999; Pruitt et al. 2000; Wellesen et al. 2001; Chen et al. 2003; Kurata et al. 2003; Baud et al. 2004; Schnurr et al. 2004; Xiao et al. 2004) appear to code for lipid-metabolizing enzymes, but their functions in cutin biosynthesis have not been fully validated. Several other genes, *ALE1*, *ACR4*, *WIN1/SHN*, *PAS2/PAP*, and *HTH*, did not appear to be directly involved in biosynthesis of the cutin polyester based on their sequence similarities and expression pattern (Tanaka et al. 2001, 2002; Bellec et al. 2002; Haberer et al. 2002; Krolikowski et al. 2003; Aharoni et al. 2004; Broun et al. 2004; Watanabe et al. 2004).

Mutants in the above-mentioned genes display pleiotropic phenotypes exhibiting cuticular defects, growth abnormalities, increased sensitivity to chemical exposures and low humidity, altered resistance to pathogens, distorted cell differentiation, illicit cell–cell interactions, and cell death (Yephremov and Schreiber 2005). Among these defects, morphological irregularities in the shape of organs and single cells represent features that suggest involvement of the cell wall, which supports the cell and determines its shape. Indeed, the bulging of epidermal cells seen in transgenic *Arabidopsis* plants expressing a secreted cutinase from *Fusarium solani* f sp. *pisi*, a lipolytic enzyme with a broad range of activity (Sieber et al. 2000), and in the loss-of-function *lacerata* (*lcr*) mutants bearing mutations in the cytochrome P450 FA ω-hydroxylase CYP86A8 (Wellesen et al. 2001) is remarkably similar to the swelling of epidermal cells observed in mutants that are impaired in the biosynthesis of the polysaccharide constituents of the cell wall (Williamson et al. 2001). *lcr* belongs to a family of cuticular mutants, including *fiddlehead* (*fdh*), that display a developmental syndrome characterized by misshapen cells and organs that occasionally display epidermal fusions between organs (Wellesen et al. 2001). A number of such mutations with abnormal epidermal fusions have been identified (Lolle et al. 1998; Tanaka et al. 2004). However, not all cuticular mutants exhibit the *lcr/fdh* syndrome; therefore, the role of cutin biosynthesis pathway in the control of cell morphology and the induction of epidermal interactions remains an open question. For example, *aberrant induction of a type three gene* (*att1*) in which the cutin content was found to be reduced to 30% bears a mutation like *lcr* in the cytochrome P450 FA ω-hydroxylase, and is morphologically identical to wild-type (WT) plants (Xiao et al. 2004).

To further understand the mechanisms that underlie the processes of cuticle formation, we report here biochemical and molecular genetic characterization of the APB24/*hth* organ fusion mutant of *Arabidopsis*. The finding that the APB24/*hth* mutant is disrupted in the oxidation of long-chain ω-hydroxy FAs to ω-oxo FAs is consistent with the central role that α-,ω-dicarboxylic FAs have been proposed to play in the formation of cuticle in *Arabidopsis*. The end products of this ω-oxidation pathway, α-,ω-dicarboxylic FAs, may not only be an integral part of the cuticle membrane in *Arabidopsis*, but may be generally required for the cross-linking that ensures the integrity of the outer epidermal cell wall.

Materials and methods

Plant material and growth conditions

The mutant seeds were generated by *En/Spm* transposon mutagenesis of *Arabidopsis thaliana* (L.) Heynh. ecotype Columbia (Col-0) as described (Wisman et al. 1998). Mutant and WT plants (maintained in culture, Max-Planck-Institut für Züchtungsforschung, Cologne, Germany) were raised in a greenhouse at 22–23°C on either an 8-h photoperiod (short day) or a 16-h photoperiod (long day) at 50–60% relative humidity.

Gel blot analysis and genotyping

DNA was isolated by the cetyltrimethylammonium bromide method from leaves of 10-week-old plants and further purified according to Qiagen protocols by using Qiagen Genomic-tip 20/G. For gel blotting, 2 μg DNA were digested with *Vsp*I (MBI Fermentas, St Leon-Rot, Germany), which we found to be most suitable for co-segregation analysis using probes for the 3′ and 5′ ends of the *En/Spm* transposon. RNA was extracted by using Total RNA reagent (Biomol, Plymouth Meeting, PA, USA). Hybridization probes were generated by using polymerase chain reaction (PCR); gel blotting and hybridization were carried out using standard protocols, except that PerfectHyb hybridization buffer (Sigma, St Louis, MO, USA) was used. The PCR genotyping was performed using the En8130 (GAGCGTCGGTCCCC-ACACTTCTATAC) transposon primer and the ACE10 (CCCGACTTCTCTCTCCTCCACTGC) and ACE11 (TCAGCCTCTGAAGCTCCTTCTTAGG) gene-specific primers flanking the insertion site.

Comparative metabolic profiling

Wild types and progeny of heterozygous plants were grown until flowering to identify *hth-12* mutants. The isolation of lipids from inflorescences and leaves and analysis was carried out as described previously (Browse et al. 1986), except that heptane was used instead of hexane. The heptane phase was transferred into a GC microvial and analyzed with a Hewlett Packard 5890 series II gas chromatograph coupled to the HP 5973 Mass Selective Detector.

An HP-5MS methyl phenyl silicone capillary column (10 m×0.20 mm) was used.

Chromatographic parameters were: injector temperature 250°C; initial oven temperature 150°C for 1 min; the temperature was then raised to 320°C at 12°C/min, and held there for 5 min. Peak areas were corrected before comparison with the area of the α-linolenic acid peak, which was used instead of an internal standard.

Analysis of residual-bound lipids

Mature leaves of flowering WT and *hth-12* mutant plants (about 300 mg per sample) were harvested and their areas measured by scanning. Soluble lipids were extracted from samples by steeping in 25 ml of methanol/chloroform (1:1, v/v) mixture for 7 days, changing the solvent daily. After drying, the leaf material was weighed (typically about 30 mg) and stored or used directly for analysis.

Transesterification of the residual-bound lipids was performed with 6 ml of 1N HCl in methanol (2 h, 80°C) in a Teflon-sealed screw-cap tube. The hydrophobic monomers were subsequently extracted into hexane (three times with 6 ml) containing 20 μg of dotriacontane (C32) as an internal standard. After evaporating the solvent to 100 μl at 50°C under a stream of N_2, free hydroxyl groups were converted into their trimethylsilyl ethers with 20 μl of *N,N*-bis-trimethylsilyltrifluoroacetamide and 20 μl of pyridine (40 min, 70°C). GC–MS analysis was carried out using a gas chromatograph 6890N equipped with a quadropole mass selective detector 5973N (Agilent Technologies, Boeblingen, Germany). Quantitative determination of lipids was carried out with the same GC system equipped with a flame ionization detector.

Transgene constructs and generation of transgenic plants

The 1.9-kb promoter fragment upstream the start ATG of *ACE/HTH* was obtained by PCR with the primers ACE-Hind (AAAAA*AAGCTT*CAAAAGAGGACTAAAGAGGAGAGAAAC) and ACE-Xba (AAAAAA*TCTAGA*CTTATGTGGCTTTTGATGAATGGTC), which introduced *Hind*III and *Xba*I cloning sites (italicized), respectively, at the 5′ and 3′ ends of the promoter.

ACE promoter–reporter binary vectors and in planta transformation were done similarly as described previously (Efremova et al. 2004).

Microscopy and in situ hybridization

Cryo-scanning electron microscopy (SEM) was performed as described previously (Yephremov et al. 1999). For transmission electron microscopy (TEM), plant materials were fixed with a mixture of glutaraldehyde (2%) and formaldehyde (4%) in sodium cacodylate (0.05M, pH 7.2) for 2 h and postfixed with OsO_4 (1%) in sodium cacodylate at 4°C overnight, dehydrated with ethanol, and embedded in LR White resin (London Resin Company Ltd., London, UK) at 60°C for 24 h. Ultrathin sections (50–100 nm) were double-stained with uranyl acetate (5%) for 30 min and Reynolds lead citrate for 2 min, and then examined with a Zeiss EM 10C microscope.

GFP fluorescence and GUS expression in transgenic plants were examined as described elsewhere (Efremova et al. 2004). The 1,600-nt probe fragment for in situ hybridization was prepared from a full-length cDNA (RIKEN cDNA clone RAFL09-23-C13) by PCR with the ACE-SP6 (*CTCGAGTTTAGGTGACACTATAGAACTGGAG*CCTCCACTGCCTCTAAAGGTAAAGAG) and ACE-T7 (*CTCGAGTAATACGACTCACTATAGGGAG*ACACCAAGAACTTTGCGGTTAGGG) primers (the SP6 and T7 promoters are italicized). In situ hybridization was performed as previously described (Efremova et al. 2004). For negative control, sections were hybridized with a digoxigenin-labeled sense probe generated from the same fragment using SP6 polymerase and no signal was found (data not shown).

Results

Floral phenotype conferred by the APB24 mutation

The recessive APB24 mutant was identified in the collection of *Arabidopsis En/Spm* transposon mutants (Wisman et al. 1998) by visual screening for infertility and an absence of silique elongation (Sorensen et al. 2003). The APB24 mutant was unable to fully unfold calyces and occasionally produced fusions between floral buds (Fig. 1a, c). However, mutant plants were indistinguishable from the WTs before flower development. Examination by SEM mostly revealed petals fused to sepals (Fig. 1d), stamens, and pistil; however, fusions between sepals were also regularly observed in mutant flowers. Despite this, no noticeable differences were found between sepal, stamen, and pistil epidermal cells in APB24 and WT plants under SEM. Petal epidermal conical cells exhibited a marked cell-morphology phenotype, which was also preserved after cryofixation without dehydration and drying. Figure 1e, f shows that the petal surface in APB24 is composed of atypical cells that are deflated in appearance, suggesting that the APB24 gene is required to achieve the proper final morphology of conical cells in the petal epidermis.

The organ fusion phenotype of the mutant was strong in the bottom flowers that remained closed (Fig. 1a), whereas in the upper third or fourth of the mutant inflorescence, weaker fusions of floral organs allowed petals to emerge (Fig. 1b, brackets). Although a range of morphological abnormalities could still be seen in petals of these upper flowers, their silique set

Fig. 1 a–l Phenotype of the APB24 *(hth-12)* transposon insertion mutant. **a** The main inflorescence of the *hth-12* mutant, from a 14-week-old plant, bearing unopened sterile flowers and showing fusions between floral buds. **b** The main shoot and axillary shoots of a 16-week-old *hth-12* with sterile flowers in the bottom and fertile flowers in the upper part (indicated by *brackets*) of the inflorescence. **c–f, l** Scanning electron micrographs, **h–k** Transmission electron micrographs. **c** Because of organ fusions, *hth-12* mutant buds do not unfold and are typically sterile. **d** Fusion between sepal and petal. **e** With electron microscopic examination, the *hth-12* phenotype is most obvious in the petal epidermis. Conical epidermal cells are misshapen and deflated that is shown in greater detail in **f** (magnified view of the *boxed area* in **e**). **g** Instability of transposon at the *hth-12* allele result in fertile flowers in the bottom of the inflorescence (*arrows*). **h–j** Cuticle proper (*arrows*) of septum is seen on electron micrographs as a dark layer above the light cell wall. In *hth-12* mutants, it may be discontinuous (**i**) or multilayered (**j**) compared to wild type (**h**). **k** Cell wall fusions between anther and petal. **l** Reverted cells (*arrows*) are not able to restore the loss of function in the neighboring cells. A sharp delineation between the reverted sector consisting of petal-typical conical cells and the mutant sector is observed suggesting that the function of *ACE/HTH* is cell autonomous. *an* anther, *ow* ovary wall, *pe* petal, *se* sepal, *sf* stamen filament, *sm* septum. *Scale bars* 10 mm (**a, b**), 500 μm (**c**), 50 μm (**d, e**), 10 μm (**f**), 20 μm (**l**), 0.1 μm (**h–j**), 0.5 μm (**k**)
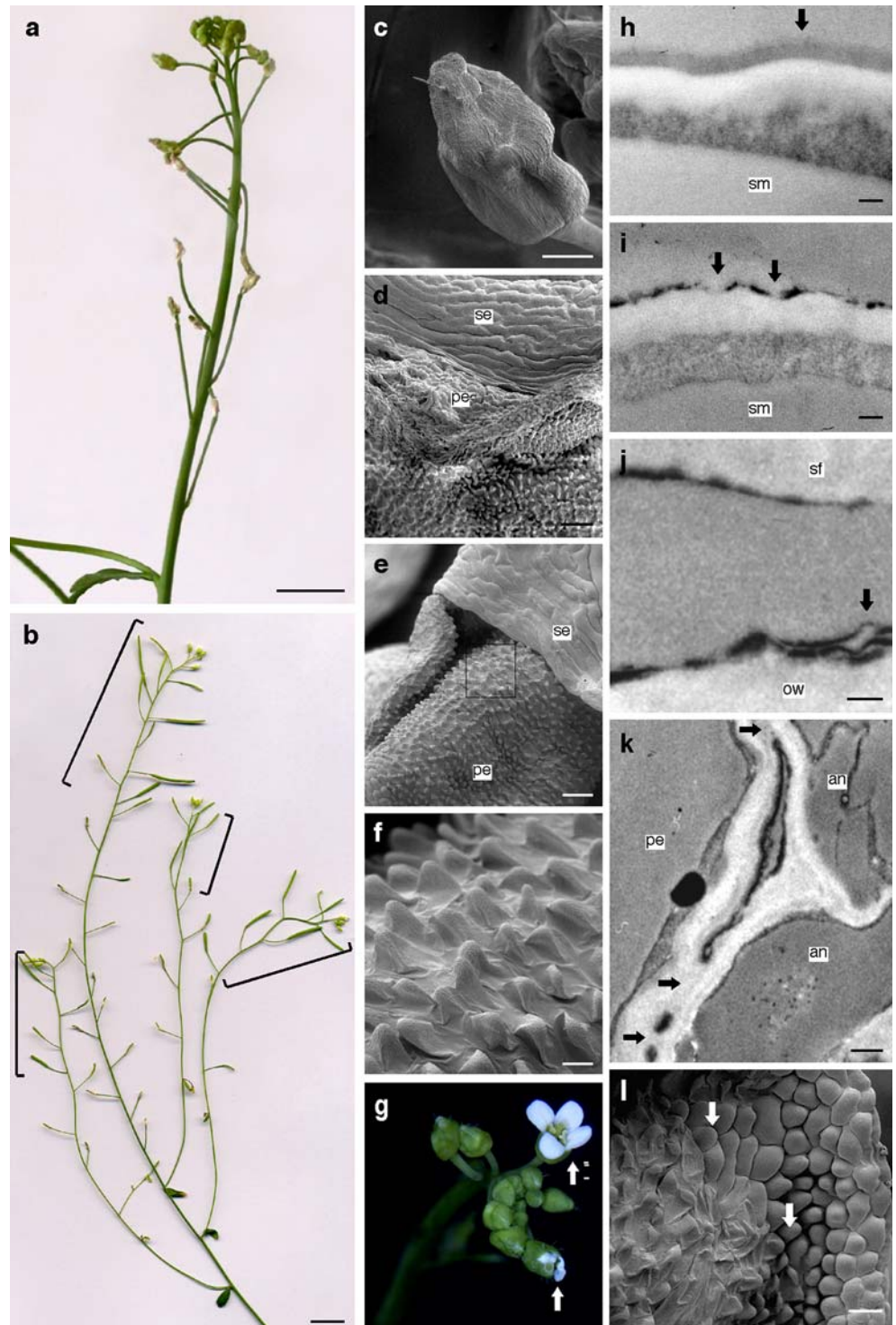
recovered to normal (Fig. 1b), and essentially all seeds gave rise to ABP24 mutant plants. In some mutant plants infrequently (0.1–7%), bottom flower buds were able to open (Fig. 1g) and to produce R_1 seeds, which gave rise to WT and mutant plants in a 3:1 ratio suggesting reversion of a transposon-induced APB24 mutant allele. The R_1 families did not always (4 out of 26 families) segregate 3:1 but rather showed an excess of mutants over WTs, indicating that some reversions of a transposon at the APB24 locus that occurred in the R_0 mutant plants led to L1 periclinal chimeras. The rate of mutants in this series was actually similar to that obtained with the *fdh* mutant caused by the insertion of the *En/Spm* transposon (Yephremov et al. 1999). However, because ABP24 mutants are not completely sterile, the reason for the excess of the mutant seeds in some R_1 families is difficult to substantiate.

Reversions of the several *En/Spm* transposon-in-duced mutant alleles in *Arabidopsis*, e.g., *dwf4-En1240* (Yephremov and Saedler 2000; A. Yephremov, unpublished data) frequently result in chimeras producing mutant and WT shoots on the same plant. Most reversions in APB24 mutants occur later and, at best, result in appearance of fully or partially open flowers in the bottom part of the mutant inflorescence. In partially open flowers, we observed transposon-induced mericlinal chimeras appeared as sectors of WT tissue of mutant petals. In the absence of an independent marker for chimeric analysis, complete discrimination between mutant and normal tissue was not possible. However, the analysis of revertant sectors under SEM shows that they have sharp borders, with cells appearing WT in the sector and the adjacent cells that are strongly deflated in appearance. This suggests that reverted WT cells cannot rescue the phenotype of neighboring mutant cells in the petal epidermis (Fig. 1l), indicating that the function of APB24 in cell morphogenesis is cell autonomous.

Thus, the genetic analysis of germinal revertants and the occurrence of mosaic tissues in the petals of the mutant demonstrate that the APB24 locus is unstable and likely to be tagged by a transposon.

Molecular cloning by transposon tagging shows that APB24 is allelic to *ace* and *hth*

For co-segregation analysis, leaf material (for DNA isolation) and seeds were collected from 41 WT plants in the four distantly related populations segregating for the reverting APB24 mutant. Heterozygous and homozygous WT plants were identified by progeny testing. Southern blots prepared from 17 heterozygous and 17 homozygous WT plants were probed with an *En/Spm* transposon probe. Five heterozygous plants were selected based on distinct restriction fragment length polymorphisms and fewer transposon insertions (5–6). After transposon flanking sequences had been amplified by TID with the 3′ end transposon primers as described (Yephremov and Saedler 2000; Steiner-Lange et al. 2001) and fractionated on an agarose gel (Fig. 2a), the single fragment common to all five plants was detected. To isolate the transposon-flanking fragment for sequencing, the TID segregation analysis was repeated with the Transgenomic WAVE system, equipped with a fraction collector, and run in non-denaturing mode at 50°C. The flanking sequence comprised a part of the *ADHESION OF CALYX EDGES* gene (Araki and Nakatani-Goto 1999), which has been published only in a database, and the *HOTHEAD* (*HTH*) gene for which 11 mutant alleles have been described (Krolikowski et al. 2003). The *En/Spm* transposon insertion occurred in the 5′-untranslated region, 19-bp upstream from the ATG start codon (Fig. 2b), and resulted in the loss of the gene-specific transcript (data not shown).

We took advantage of germinal revertants of the *En/Spm*-induced recessive APB24 allele, because in this case
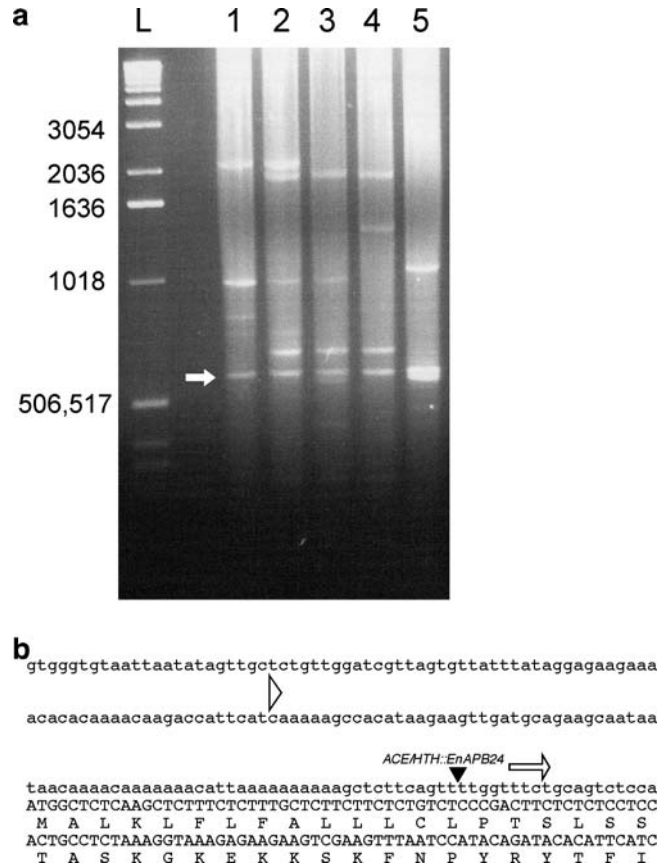

Fig. 2 a–b Cloning of the *hth-12* allele by transposon tagging. **a** Segregation analysis of TID-amplified flanking sequences in a 1.5% agarose gel. The band common to all heterozygous plants (1–5; indicated by the *arrow*) represents a PCR fragment derived from the *hth-12* mutant locus. The sizes of the DNA fragments (in bp) in the 1-kb DNA ladder are given on the left. **b** Structure of the 5′ end of the *hth-12* mutant allele containing the *En/Spm* transposon insertion. The deduced amino acid sequence of *ACE/HTH* is shown below the nucleotide sequence. The position of the putative transcription start, based on the longest cDNA clone obtained so far, is indicated by the *arrowhead*. The location of *En/Spm* insertion is shown by the *black triangle*. The *arrow* shows the orientation of the transposon

co-segregation analysis makes it possible to prove conclusively that a given mutant phenotype is caused by the transposon insertion in the gene. For co-segregation analysis in two revertant families, R_1 WT and mutant plants, segregating in a 3:1 ratio, were genotyped by PCR using transposon and *HTH* gene-specific primers flanking the insertion site. Genotypes of R_1 WT parents were proven by performing progeny testing for the organ fusion phenotype in the R_2 generation. Thereby, we confirmed that the APB24 mutant phenotype was the result of *En/Spm* inserting in the *HTH* gene and not from another mutation. Thus, the APB24 allele was denoted *hth-12*. The morphological aspects of the *hth-12* phenotype, including organ fusion, sterility, and the absence of defects in trichome development were similar to those reported for *hth* mutants carrying stronger alleles (Lolle et al. 1998; Krolikowski et al. 2003).

ace/hth exhibits structural defects in the cuticle

The organ fusion phenotype of *ace/hth* is shared by a class of mutants in *Arabidopsis* described previously (Lolle et al. 1998). Although the relations between fusion phenotypes and cuticle properties remain controversial, it is commonly accepted that an ability to produce epidermal fusions is linked to cuticle defects because, beside fusions, this class of mutants is characterized by increased rate at which chlorophyll could be extracted from rosette leaves as a measure of cell wall and cuticle permeability and pollen germination on non-reproductive organs (Lolle et al. 1998).

However, direct examination of the cuticle in the *ace/hth* mutants has not been reported. Because the mutant phenotype of *hth-12*, quite strong in inflorescences, was neither expressive nor fully penetrant before flower development, we examined the epidermis of floral buds by TEM.

In the WT, the cuticle appears in micrographs as a regular darker-colored layer on the outer surface of epidermal cell walls (Fig. 1h). Compared to WT, cuticle in the mutant was marked by breaks; intermittent areas were alternated with multilayered patterns formed by darkly stained cuticular polymers intervening lightly stained areas of the cell wall (Fig. 1i–k). These changes were most conspicuous in petals and at the inner epidermis of the pistil, including the septum and ovules, but were not observed in sections of sepals. In organ fusion zones (Fig. 1k, arrows), the cell walls of both epidermal cells came into direct contact, and electron-dense structures corresponding to the cuticle proper were not detected.

Comparative metabolic profiling reveals that *hth-12* is defective in the oxidation of long-chain ω-hydroxy FAs to ω-oxo FAs

The mixed-layer structure of the cuticle in *hth-12* resembles that of *Arabidopsis* transgenic plants expressing a secreted cutinase from *F. solani* f sp. *pisi* (Sieber et al. 2000) and suggests that the *hth* mutation directly or indirectly affects the ability of plants to form the continuous cuticle proper. Its major component, cutin, can be hydrolyzed in *Arabidopsis* into a mixture of C16 and C18 monomers, with α-,ω-dicarboxylic and hydroxy FAs as its major components (Bonaventure et al. 2004; Yephremov et al. 2004; Xiao et al. 2004; Franke et al. 2005).

Therefore, in order to identify the molecular mechanism underlying the cuticular defects in *hth-12*, we analyzed the lipid metabolites present in inflorescences by gas chromatography (GC) coupled with mass spectrometry (MS). We reasoned that because the *hth-12* phenotype is prominent only in inflorescences and the *ACE/HTH* gene is highly expressed in stems and inflorescences (Krolikowski et al. 2003), tissue samples prepared from this organ would be most suitable for biochemical analysis. We postulated that if ACE/HTH is directly or indirectly involved in FA metabolism, loss of its activity in the mutant should result in an accumulation of its substrate and a decrease in its product, when compared to the WT.

To exclude possible influence of background mutations, total lipids were extracted for comparison from inflorescences of *hth-12* and WT plants segregating in the same families. Ten plants of each phenotype taken from four families were pooled and analyzed for FA composition. FA metabolites were identified by their retention times and from their mass spectra, and the ratios of peak areas in *hth-12* and WT were compared (Fig. 3a). While ratios close to 1 were obtained for most of the compounds, the ratios for five metabolites were altered by up to twofold. To establish the molecular identities of these metabolites, their mass spectra were compared to those of reference substances in mass spectra libraries. One compound showed a marked increase in the *hth-12* mutant and was identified as 18-hydroxyoctadecadienoic acid (Fig. 3a, peak 3), while ω-oxo FAs with aliphatic chains of 16 and 18 carbons in length (Fig. 3a, peaks 2 and 5, respectively) were present in reduced amounts. The other compounds whose levels were lower in the mutant were the end products of ω-oxidation—C16 and C18 α-,ω-dicarboxylic acids (Fig. 3a, peaks 1 and 4, respectively). Parallel experiments with leaf samples showed similar results (data not shown) but greater differences between WTs and mutants were observed from the inflorescence samples. This is consistent with the increased expression of *ACE/HTH* in stems and inflorescences relative to leaves as shown by reverse transcription (RT-PCR; Krolikowski et al. 2003). These results are direct chemical indications that the *hth-12* mutant is defective in the oxidation of long-chain ω-hydroxy FAs to ω-oxo FAs.

hth-12 is defective in the biosynthesis of major long-chain α-,ω-dicarboxylic FAs in cell wall- and cuticle-bound lipids

We proposed that if the *ace/hth* mutation has an adverse effect on the formation of the cuticle proper and oxidation of long-chain ω-hydroxy FAs to ω-oxo FAs, it should be possible to detect the reduction in the levels of α-,ω-dicarboxylic FAs in the insoluble polymeric material isolated from the *hth-12* mutant. This approach is similar to the one used by Bonaventure et al. (2004) and Franke et al. (2005), who also discussed the technical aspects of the method.

For this analysis, leaves from WT and mutant plants showing no reversions in the bottom part of the mutant inflorescence were collected and optically scanned, thus allowing a quantitative measurement of cuticular lipids to be expressed in terms of weight per unit area. The leaves were thoroughly steeped in organic solvents to extract all soluble lipids. After several days of extraction, the remaining polyester lipids were subjected to hydrolysis,
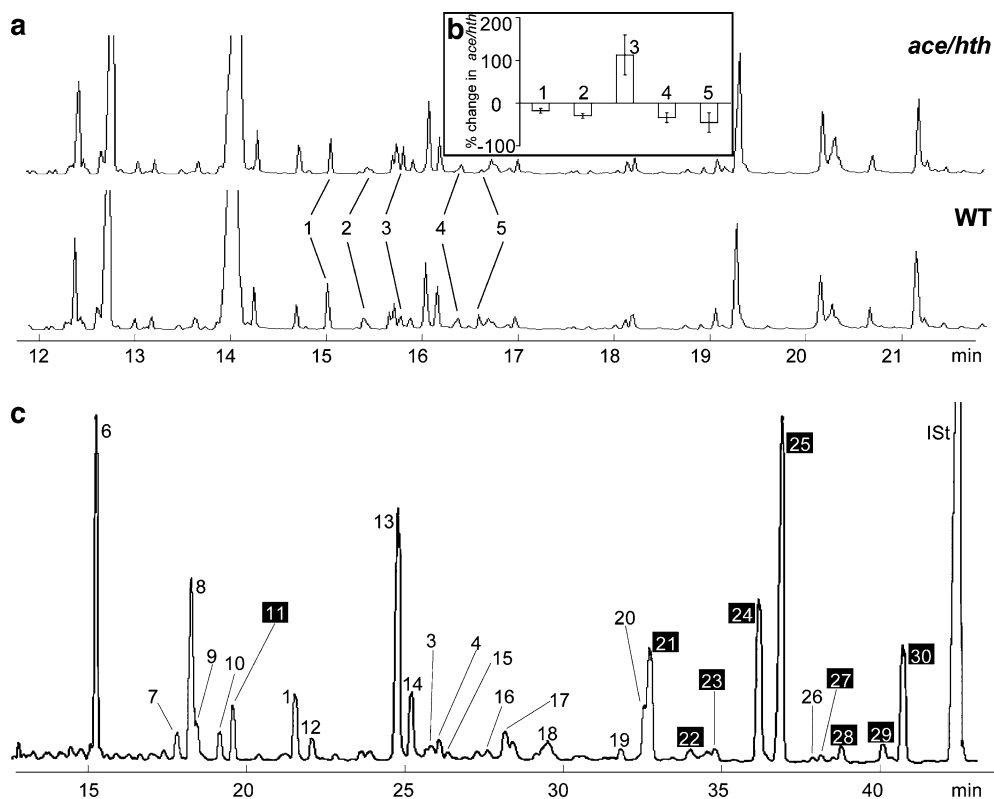
Fig. 3 a–c Gas chromatography–mass spectrometry analysis of FA metabolites. **a** Comparative metabolic profiling of total lipids extracted from *hth-12* and wild-type (WT) inflorescences. **b** Five metabolites (peaks 1–5), the accumulation of which is affected in *hth-12*, are shown as mean (±SE) percentage changes (*n* = 3). **c** Metabolic profiling of residual-bound lipids extracted from WT mature leaves. The *white numbers on black background* indicate the peaks corresponding to 2-hydroxy FAs. Peak identities in (**a–c**): *1* hexadecane-1,16-dioic acid; *2* 16-oxo hexadecanoic acid; *3* 18-hydroxy octadecadienoic acid; *4* octadecane-1,18-dioic acid; *5* 18-oxo hexadecanoic acid; *6* hexadecanoic acid; *7* heptadecanoic acid; *8* octadecadienoic acid; *9* octadecenoic acid; *10* octadecanoic acid; *11* 2-hydroxy-hexadecanoic acid; *12* 16-hydroxy hexadecanoic acid; *13* octadecadien-1,18-dioic acid; *14* octadecene-1,18-dioic acid; *15* 18-hydroxy octadecenoic acid; *16* 9[10]-hydroxy-hexadecane-1,16-dioic acid; *17* docosanoic acid; *18* tricosanoic acid; *19* tetracosenoic acid; *20* tetracosanoic acid; *21* 2-hydroxy-docosanoic acid; *22* 2-hydroxy-tricosenoic acid; *23* 2-hydroxy-tricosanoic acid; *24* 2-hydroxy-tetracosenoic acid; *25* 2-hydroxy-tetracosanoic acid; *26* hexacosanol; *27* 2-hydroxy-pentacosenoic acid; *28* 2-hydroxy-pentacosanoic acid; *29* 2-hydroxy-hexacosenoic acid; *30* 2-hydroxy-hexacosanoic acid; *first*, internal standard

derivatized, and analyzed by GC–MS. A typical chromatogram obtained for WT (Fig. 3c) demonstrates the separation and peak identities of the long-chain FA derivatives identified by the mass spectra data. The chromatogram in Fig. 3c shows that only a few minor peaks remain unidentified. The two major classes of compounds that constitute residual-bound lipids in *Arabidopsis* leaves are α-,ω-dicarboxylic C18 and C16 FAs and 2-hydroxy C24 FAs. C18 (2) and C16 FAs are also present but in smaller quantities, whereas ω-hydroxy FAs are relatively minor components of the total residual-bound lipid pool.

In the leaf polyesters isolated from the *hth-12* mutant, lower than normal levels of α-,ω-dicarboxylic FAs ($P < 0.01$) and elevated levels of ω-hydroxy FAs ($P < 0.05$) were identified (Table 1). This is in agreement with the idea that *hth-12* is deficient in the long-chain FA ω-alcohol dehydrogenase activity, which is required for biosynthesis of α-,ω-dicarboxylic FAs in leaf polyesters. The amount of other major components, e.g., FAs and 2-hydroxy FAs, determined by GC–MS, generally remained unchanged in *hth-12* or was slightly lower than normal, although the vast majority of differences were not significant at the 0.05 level. The total amount of residual-bound lipids was insignificantly decreased in *hth-12* ($P < 0.36$). It is worth noting that the observed differences between *hth-12* and WT may be masked to some extent due to somatic reversions to the ACE/HTH allele in some *hth-12* cells, and the difference between the two may actually be a few percent higher.

Epidermis-specific expression pattern of *ACE/HTH* agrees with the cuticular phenotype of *hth-12*

In plants, α-,ω-dicarboxylic FAs were found in high proportion in specialized tissues, such as endodermis of roots and the epidermis, which prevent or restrict apoplastic transport of water and solutes or protect underlying tissues (Kolattukudy 2001c). However, the ubiquitous expression of *ACE/HTH* in all tissues and cell types as has been reported previously (Krolikowski

Table 1 Fatty acid composition analysis of residual-bound lipids in *hth-12* and wild type

Peak ID[a]	Compound	*hth-12*, ng/cm^2		WT Col, ng/cm^2		Difference between *hth-12* and WT Col[b]
		Mean ($n=6$)	±SE	Mean ($n=5$)	±SE	
	Acids					
6	Hexadecanoic acid (C16)	112.61	5.35	114.60	8.26	
7	Heptadecanoic acid (C17)	4.93	0.91	3.40	0.24	
8	Ocadecadienoic acid [C18(2)]	122.35	2.53	126.24	9.32	
9	Ocadecenoic acid [C18(1)]	10.61	1.26	13.63	1.59	
10	Octadecanoic acid (C18)	10.03	1.43	10.96	1.75	
17	Docosanoic acid (C22)	14.34	0.47	16.02	0.89	
18	Tricosanoic acid (C23)	4.89	0.85	7.67	2.65	
19	Tetracosenoic acid [C24(1)]	11.30	0.34	13.11	0.89	
20	Tetracosanoic acid (C24)	36.88	1.48	38.30	2.07	
	Total	327.94	11.24	343.92	27.52	
	Primary alcohols					
26	Hexacosanol (C26)	6.31	0.34	5.97	0.95	
	ω-Hydroxyacids					
12	16-Hydroxyhexadecanoic acid (C16)	15.81	1.73	10.25	0.93	I; $P<0.01$
15	18-Hydroxyoctadecenoic acid [C18(1)]	8.89	1.59	9.41	0.74	
3	18-Hydroxyoctadecadienoic acid [C18(2)]	19.92	0.92	12.99	2.64	I; $P<0.02$
	Total	44.63	1.92	32.65	4.71	I; $P<0.05$
	α-,ω-Dicarboxylic acids					
1	Hexadecane-1,16-dioic acid (C16)	100.92	1.86	120.00	9.66	
14	Octadecene-1,18-dioic acid [C18(1)]	54.76	2.04	70.20	4.11	D; $P<0.01$
13	Octadecadiene-1,18-dioic acid [C18(2)]	283.89	8.78	386.52	20.02	D; $P<0.01$
4	Octadecane-1,18-dioic acid (C18)	15.15	2.58	22.19	1.86	
	Total	454.71	16.03	598.90	39.26	D; $P<0.1$
	2-Hydroxyacids					
11	2-Hydroxy-hexadecanoic acid (C16)	17.16	1.60	15.42	1.06	
21	2-Hydroxy-docosanoic acid (C22)	50.92	2.37	55.61	4.12	
22	2-Hydroxy-tricosenoic acid [C23(1)]	7.80	1.02	9.42	1.25	
23	2-Hydroxy-tricosanoic acid (C23)	9.83	0.74	14.79	2.21	
24	2-Hydroxy-tetracosenoic acid [C24(1)]	158.66	3.43	173.40	11.47	
25	2-Hydroxy-tetracosanoic acid (C24)	211.61	5.14	227.35	13.60	
27	2-Hydroxy-pentacosenoic acid [C25(1)]	11.69	0.26	14.50	1.11	
28	2-Hydroxy-pentacosanoic acid (C25)	13.22	0.24	16.65	1.11	D; $P<0.03$
29	2-Hydroxy-hexacosenoic acid [C26(1)]	22.21	0.49	23.51	1.65	
30	2-Hydroxy-hexacosanoic acid (C26)	62.73	1.00	66.79	3.37	
	Total	565.82	18.13	617.44	44.40	
	Mid-chain oxygenated hydroxyacids					
16	9(10),16-Dihydroxyhexadecanoic acid (C16)	7.70	1.10	10.83	0.98	D; $P<0.04$
	Total	1,399.41	111.88	1,598.89	45.68	

P values greater than 0.05 are not shown

SE standard error, *D* decrease, *I* increase

[a] Peak identities in Fig. 3c

[b] Difference: *hth-12* versus wild-type Columbia (WT Col) by Mann–Whitney non-parametric test

et al. 2003) strongly suggests that the activity of *ACE/HTH* does not specifically control the epidermis-specific biosynthetic pathways, including the biosynthesis of α-,ω-dicarboxylic FAs, but rather seems to be involved in distinct biochemical processes.

To examine the expression of the *ACE/HTH* gene in more detail in cells where α-,ω-dicarboxylic FAs are not produced, we generated *ACE/HTH*::GFP and *ACE/HTH*::GUS promoter–reporter gene fusions in transgenic plants, since this method is often more sensitive than the in situ hybridization technique used in the earlier study (Krolikowski et al. 2003). Unexpectedly, expression of *ACE/HTH* was found with this method to be specific to the protoderm and epidermis in all vegetative and generative organs (Fig. 4a–f). This result is in disagreement with that reported by Krolikowski et al. (2003).

To test that this discrepancy was not due to missing essential promoter sequence elements in the *ACE/HTH* promoter–reporter gene fusions, we performed mRNA in situ hybridization with WT plants using anti-sense *ACE/HTH* RNA as a digoxigenin-labeled probe. After hybridization, incubation with anti-digoxigenin antibodies conjugated to alkaline phosphatase and staining, a dark blue precipitate was observed at the hybridization sites. In all organs examined, the expression pattern of ACE/HTH was epidermis specific (Fig. 5), thus validating the accuracy of the promoter–reporter analysis.

Both methods, promoter–reporter analysis and mRNA in situ hybridization, provide agreement that expression of *ACE/HTH* tends to be stronger in epidermal cells of young and actively growing vegetative and floral organs. *ACE/HTH* transcripts were detected in the L1 cell layers of vegetative apical meristems and
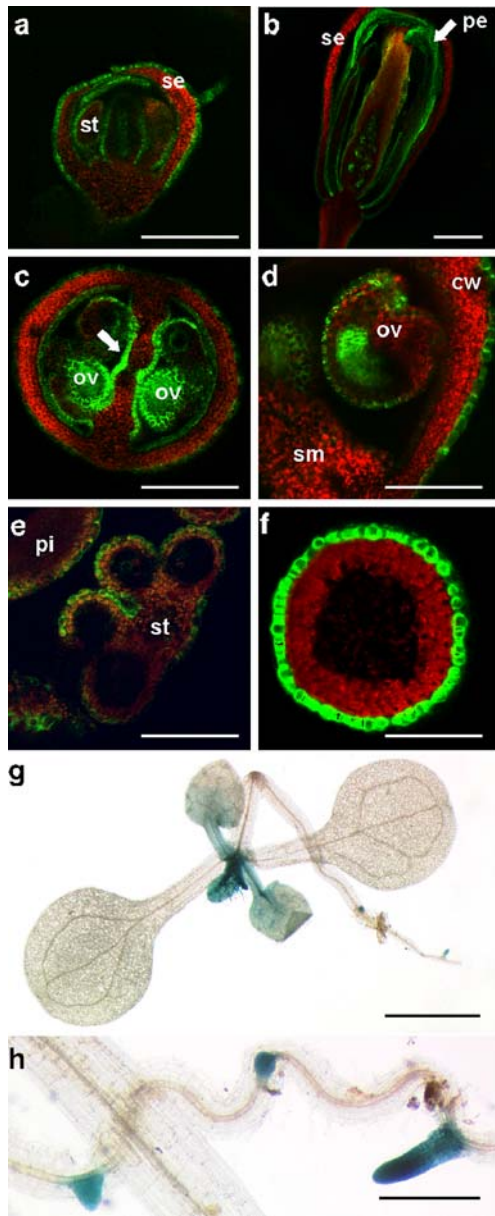
Fig. 4 a–h Tissue-specific expression of *ACE/HTH*. **a–f** GFP expression driven by the *ACE/HTH* promoter in transgenic plants. **a** and **b** Longitudinal sections through floral buds showing that, although *ACE/HTH* is expressed in all floral organs, it is relatively strongly expressed in petals in mature buds (**b**, *arrow*). **c** and **d** Cross-section through the central part of the pistil shows the obvious expression in the septum (*arrow*) and ovules (**d**). **e** Cross-sections through anther. **f** Cross-sections through pedicle (flower stalk). **g** and **h** GUS reporter gene expression under the control of the *ACE/HTH* promoter in four-leaf seedlings is centered in the shoot apical meristem and young leaves (**g**) and it can be observed in root initials (**h**). *ov* ovule, *ow* ovary wall, *pe* petal, *pi* pistil, *se* sepal, *sm* septum, *st* stamen. *Scale bars* 200 μm (**a, c, f, h**), 100 μm (**d, e**), 400 μm (**b**), 2 mm (**g**)

first leaves, but its accumulation decreased in older leaves (Fig. 5a). Accordingly, most of the GUS staining in *ACE/HTH::GUS* plants was observed in young, developing leaves (Fig. 4g). In situ hybridization experiments revealed the expression of *ACE/HTH* in
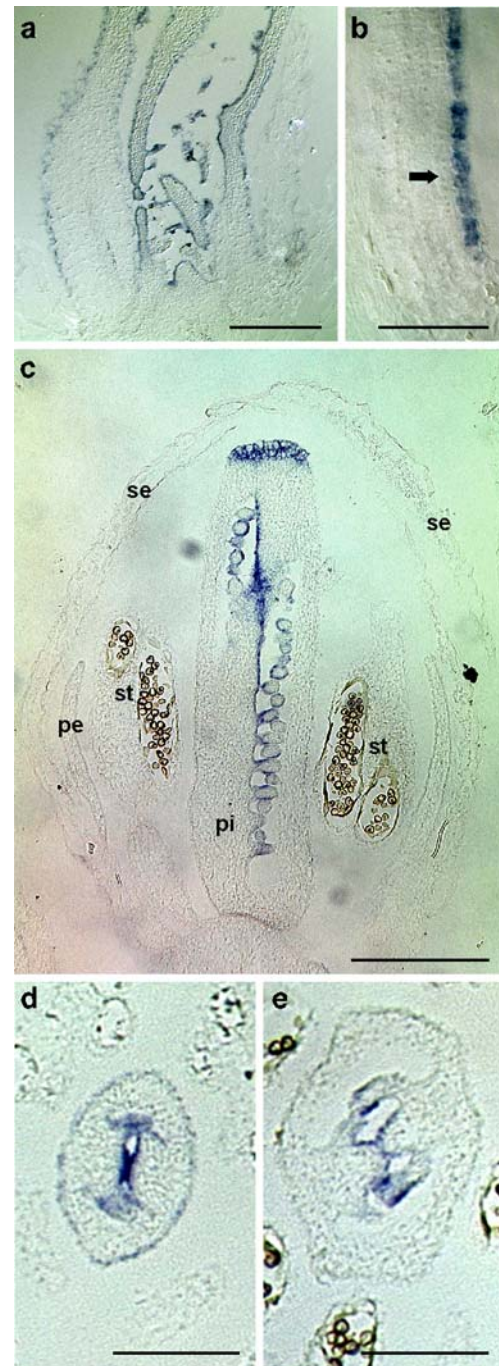

Fig. 5 a–e In situ hybridization with wild-type vegetative and floral tissues using DIG-labeled anti-sense probe of *ACE/HTH*. *Dark blue signals* indicate the presence of the *ACE/HTH* transcript in epidermal cells. **a** Longitudinal section through the vegetative apex of a 10-day-old plant. Note that *ACE/HTH* mRNA is expressed in the protodermis. **b** Higher magnification of the epidermis (*arrow*) on longitudinal section through the stem of an 6-week-old plant; *ACE/HTH* continued to be strongly expressed at later stages of development in the epidermis of the stem. **c** Mature floral bud. Notice that expression of *ACE/HTH* can hardly be detected in sepals, petals, and stamens at this stage, but is apparently strong in the septum, ovules, and stigma. In younger buds, expression was observed in all of these organs (data not shown); *pe* petal, *pi* pistil, *se* sepal, *st* stamen. **d** and **e** Cross-sections through developing pistils at the beginning of postgenital carpel fusion (**d**) and at the more evolved stage (**e**). *Scale bars* 100 μm (**a**), 50 μm (**b, d, e**), 200 μm (**c**)

prefusion epidermal cells of carpels and ovule primordia (Fig. 5c–e). The adaxial epidermis of carpels showed conspicuous expression of *ACE/HTH* only at early developmental stages (Fig. 5d), whereas the adaxial epidermal cells maintained high transcript levels throughout pistil development. Finally, high expression levels of the *ACE/HTH::GFP* gene fusion were detected in young buds in all floral organs (Fig. 4a), including sepals, whereas strong GFP signal was seen only in petals and ovules at later developmental stages (Fig. 4b).

Similar to *FDH* (Efremova et al. 2004), *ACE/HTH* is expressed in ovule integuments (Fig. 4d), which share a common L1 origin with epidermal cells. The *ACE/HTH* promoter–GFP reporter transgenic plants showed a remarkable fluorescence signal in the septum epidermal cells (Fig. 4c), showing that the direction of regulation for the *ACE/HTH* promoter is opposite to that of *FDH*, which is downregulated in these cells (Efremova et al. 2004). Still, in many respects, the pattern of epidermis-specific expression of *ACE/HTH* in shoot tissues is similar to that of *FDH*.

The *ACE/HTH* promoter is also active in root epidermal cells (Fig. 4g, h), corroborating the results obtained in RT-PCR experiments that *ACE/HTH* is expressed in roots (Krolikowski et al. 2003).

Thus, the expression analysis of *ACE/HTH* showed that the activity of this gene appears to be under developmental control and is epidermis specific. Therefore, epidermal cells must account for the differences in the accumulation of metabolites between the *hth-12* mutant and WT. As the expression patterns of ACE/HTH determined by in situ hybridization and by promoter–reporter gene fusions are similar, this suggests that the 1.9-kb promoter fragment used in this study contains all of the regulatory elements necessary for proper expression of *ACE/HTH*.

Discussion

ace/hth is a cuticular mutant defective in the biosynthesis of major cuticular monomers

The occurrence of organ fusions which represent a major visible phenotype, increased rate of chlorophyll extraction from rosette leaves, and pollen germination on non-reproductive organs of *hth* (Lolle et al. 1998) suggested that this mutant is defective in the maintenance of the epidermis barrier function. The major extracellular barrier on the surface of aerial organs consists of cuticular lipid molecules constituting solid wax and continuous polymeric matrix. Visual inspection and biochemical analysis (data not shown) showed that the *hth* mutant secretes normal levels of epicuticular wax. This is in agreement with the apparent absence of any explicit correlation between the wax levels and organ fusions in mutants of maize and *Arabidopsis* (Yephremov et al. 1999). The notion that *hth* is impaired in the biosynthesis of cuticular polyesters is supported by

two lines of evidence. First, direct examination under TEM (Fig. 1i–k) revealed severe changes in the structure of the cuticular layer of the cell wall and the cuticle proper in the *hth-12* mutant. The presence of these changes in petals, septum, and ovules correlates well with the higher expression of *ACE/HTH* in these organs observed using in situ hybridization and promoter–GFP fusion transformants. With regard to structural changes in the cuticle, which may be discontinuous or multi-layered in the mutant (Fig. 1i, j), *ace/hth* is distinct from the other characterized cuticular mutants of *Arabidopsis*, e.g., *att1*, *wax2/yre*, *lacs2* (Chen et al. 2003; Kurata et al. 2003; Schnurr et al. 2004; Xiao et al. 2004), and is more reminiscent to cutinase-expressing plants (Sieber et al. 2000). Second, the GC/MS analysis of leaf residual-bound lipids found that *hth-12* was 25–30% reduced in the amount of α-,ω-dicarboxylic FAs as compared with WT plants (Table 1). In elegant experiments, Bonaventure et al. (2004) manually dissected under a microscope the epidermis from WT stems and demonstrated that C18:2 and C18:1 derivatives exist primarily as dicarboxylic acids in the polyesters of the epidermis and that the depolymerization products, particularly dicarboxylic acids, obtained from *Arabidopsis* leaf and stem residues originate from polyesters deposited by epidermal cells rather than underlying tissues. Pure preparations of cutin from leaves of *Arabidopsis* were obtained by using polysaccharide hydrolases. Analysis of depolymerization products showed that α-,ω-dicarboxylic FAs constitute 40% of FAs in *Arabidopsis* cutin (Franke et al. 2005).

Using in situ hybridization and GFP fusions, we found that *ACE/HTH* is apparently only expressed in the epidermis. Taken together, this strongly suggests that the changes in the amount of α-,ω-dicarboxylic FAs in *hth-12* may be attributed to the different composition of cuticular polyesters. These data are in a good agreement with previous experiments which show that de-esterifiable α-,ω-dicarboxylic FAs are an integral part of the cuticular layer of the cell wall and/or the cuticle membrane in *Arabidopsis* (Bonaventure et al. 2004; Xiao et al. 2004; Yephremov et al. 2004; Franke et al. 2005).

Putative function of ACE/HTH and functional specialization of long-chain FA ω-oxidation enzymes

Using metabolic profiling, we compared FA composition of tissues from the *hth-12* cuticular mutants and WT plants of *Arabidopsis*. We found that *hth-12* is deficient in the ability to oxidize long-chain ω-hydroxy FAs to ω-oxo FAs, and thus provided genetic evidence in plants that ω-alcohol dehydrogenase functions in the FA ω-oxidation pathway as the catalytic step after FA ω-hydroxylase. Furthermore, we found in leaf residual-bound lipids of the *hth-12* mutant, a decreased amount (about 70–80% of WT) of the end products of this pathway, including α-,ω-dicarboxylic FAs, which are the major constituents of cuticular polyesters (Bonaventure

et al. 2004; Yephremov et al. 2004) and cutin (Franke et al. 2005).

The absence of visible phenotype in the shoot organs of *hth-12*, including leaves and stems where the *ACE/HTH* gene is expressed, and the moderate level of reduction offers the possibility that another route of biosynthesis of α-,ω-dicarboxylic FAs occurs via cytochrome P450 FA ω-hydroxylases, e.g., CYP94A5-like (Le Bouquin et al. 2001), which are able to catalyze in vitro sequential reactions oxidizing the ω-terminal methyl group to the corresponding carboxyl. It is also possible that the corresponding ω-alcohol dehydrogenase share redundant functions in oxidation of constituents of cuticular polyesters with other family members.

Upon molecular cloning and sequencing, ACE/HTH was found to be a single-domain protein related to GMC (glucose–methanol–choline) oxidoreductase (pfam00732) domain-containing proteins (Krolikowski et al. 2003). Members of the GMC oxidoreductase superfamily are capable of metabolizing a wide variety of substrates and include oxidoreductases, dehydrogenases, lyases, and oxidases. They typically catalyze the oxidation of non-activated alcohols yielding an aldehyde or ketone (Dreveny et al. 2001), suggesting a possible involvement of ACE/HTH in the oxidation of fatty alcohols. ACE/HTH has about 25% sequence identity and about 40% sequence similarity with fungal alcohol oxidases including long-chain FA ω-alcohol dehydrogenases from *Candida* species that possess protein domain organization identical to that of ACE/HTH (Vanhanen et al. 2000). Biochemical evidence for the presence of a wound-induced ω-hydroxy FA dehydrogenase required for biosynthesis of α-,ω-dicarboxylic FAs in plants has been reported previously (Agrawal and Kolattukudy 1977); therefore, we hypothesized that ACE/HTH is a long-chain ω-hydroxy FA dehydrogenase. Considering that *lcr* and *att1* show features typical of cuticular mutants, and the corresponding genes code for closely related cytochrome P450 FA ω-hydroxylases, CYP86A8 and CYP86A2, respectively, ACE/HTH may catalyze the next step after LCR and ATT1 in the FA ω-oxidation pathway, and act before as yet unidentified long-chain ω-aldehyde dehydrogenases (Fig. 6).

The expression pattern of the *ACE/HTH* gene in shoots and roots (Figs. 4, 5) suggests to us that ACE/HTH is specifically required for biosynthesis of epidermis-specific extracellular matrix polymers, such as cutin. The comparative metabolic profiling did not reveal a defect in the oxidation of long-chain alcohols in the *hth-12* mutant (Fig. 3a) suggesting that if *ACE/HTH* is a long-chain FA ω-alcohol dehydrogenase, it is likely to be specifically involved in the oxidation of ω-hydroxy FAs. However we cannot exclude that ACE/HTH-like proteins, group A4 in particular (Fig. 7), are able to metabolize long-chain alcohols. This is similar to what has been observed for animal alcohol dehydrogenases, which are capable of oxidizing aliphatic alcohols and ω-hydroxy FAs (Holmquist and Vallee 1991). It is also feasible that other classes of substrates may be utilized
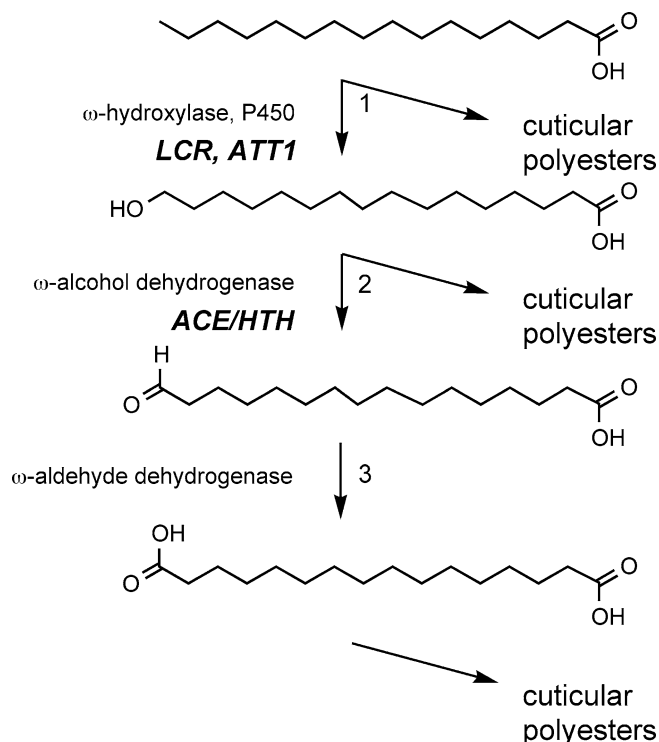

Fig. 6 Proposed FA ω-oxidation pathway for biosynthesis of cuticular polyesters in *Arabidopsis*. ACE/HTH may also act on other substrates but, for simplicity's sake, other routes except through palmitic (C16:0) acid are not shown. Biosynthetic step 1 is probably common to all plant species, while the roles of steps 2 and 3 are species specific. A parallel pathway through a cytochrome oxidase capable of performing reactions 1–3 may contribute to the amount of α-,ω-dicarboxylic FAs in cuticular polyesters

by ACE/HTH-like proteins. Functional expression of *ACE/HTH* and the *ACE/HTH*-like genes in heterologous systems is required to verify such a proposed function. Nevertheless, given that the mutant phenotype of *hth-12* as well as that of other *hth* alleles described so far (Lolle et al. 1998; Krolikowski et al. 2003) is not clearly visible in leaves and roots (data not shown), at least some of the most closely related proteins to ACE/HTH may play redundant roles in the biosynthesis of epidermal cell wall-bound polymers. A high proportion of α-,ω-dicarboxylic FAs in suberin makes it likely that other members of this family function as long-chain FA ω-alcohol dehydrogenases in the biosynthesis of suberin in the endodermis and the epidermis of roots. To test these predictions, suberin composition can be analyzed in T-DNA or transposon insertion mutants that do not express corresponding proteins.

Sequence searches in databases revealed four GMC oxidoreductase domain-containing proteins of *Arabidopsis* (Fig. 7, group A1) which share extensive homology to each other and to long-chain FA ω-alcohol dehydrogenases from *Candida* species (Fig. 7, group C). These *Candida* enzymes are involved in metabolizing FAs consumed from the medium. One of the group A1 proteins, AtFAO3/At3g23410, was successfully overexpressed in
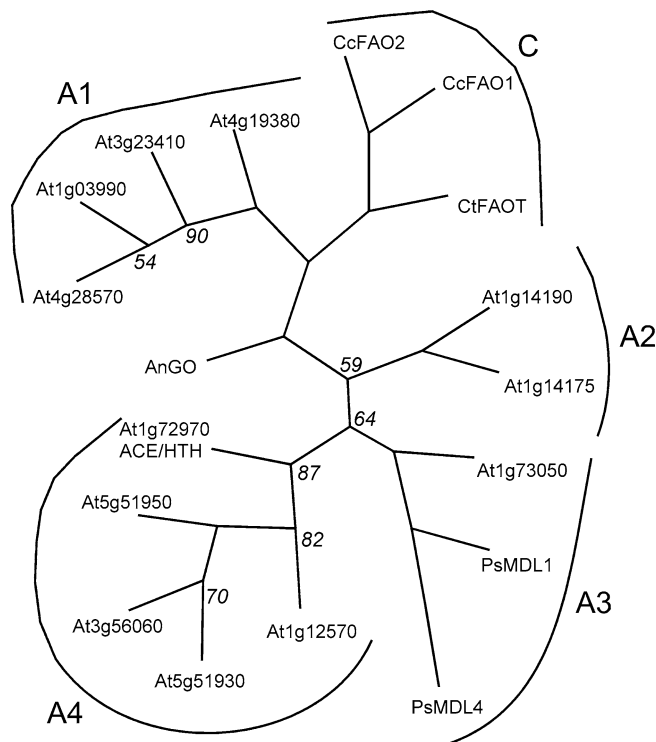
Fig. 7 The phylogenetic tree constructed from the alignment of putative long-chain FA ω-alcohol dehydrogenases and related GMC (glucose–methanol–choline) oxidoreductases. The consensus phylogenetic tree was obtained with bootstrapping using programs in the PHYLIP package as described (adapted from Efremova et al. 2004); lengths of horizontal branches are proportional to distances. The numbers at the branches are bootstrap values provided as percents over 1,000 replications; values greater than 95% are not reported. Four groups of genes can be defined in *Arabidopsis*: (1) Group A1, which is closely related to corresponding genes in the *Candida* species (C), comprises long-chain fatty-acid alcohol oxidases capable of oxidazing α-,ω-diols and, probably, ω-hydroxy FAs. (2) Group A2, includes two proteins of unknown function. (3) Group A3 is represented by mandelonitrile lyase-like At1g73050. (4) Group A4 comprises five proteins, including ACE/HTH, that are putative long-chain FA ω-alcohol dehydrogenases involved in cutin and suberin biosynthesis. *Arabidopsis* protein sequences are indicated by AGI (*Arabidopsis* Genome Initiative) gene codes. GenBank accession numbers for non-*Arabidopsis* protein sequences are: glucose oxidase AnGO: 1CF3_A; long-chain fatty alcohol oxidases CcFao1: CAB75351; CcFao2: CAB75352; CtFaot: CAB75353; mandelonitrile lyases PsMDL1: CAA69388; PsMDL4: CAA51194. *An Aspergillus niger, Cc Candida cloacae, Ct Candida tropicalis, Ps Prunus serotina*

Escherichia coli and shown to functionally express long-chain alcohol oxidase activity (Cheng et al. 2004). It seems likely, therefore, that they represent the corresponding catabolic enzymes involved in the classical ω-oxidation pathway in *Arabidopsis* that is coupled to β-oxidation in peroxisomes.

Possible role of α-,ω-dicarboxylic FAs in the fortification of the epidermal cell wall

The data presented in this paper suggest that α-,ω-dicarboxylic FAs constitute about 35–37% of the total amount of cell wall-bound lipids in WT *Arabidopsis*. This is slightly higher than the 25–30% value previously reported by Bonaventure et al. (2004) but still in the same range. Furthermore, the recent data suggest that long-chain α-,ω-dicarboxylic FAs are a specific integral part of the cutin polyester in *Arabidopsis* (Yephremov et al. 2004; Franke et al. 2005).

It was also proposed that long-chain α-,ω-dicarboxylic FAs represent a part of an underlying "suberin-like" network present in the secondary cell wall (Bonaventure et al. 2004) or required for the cross-linking that ensures the integrity of the primary cell wall (Yephremov et al. 2004). Clearly, additional data are needed to resolve this uncertainty. Nevertheless, with regard to the presence of α-,ω-dicarboxylic FAs, the composition of epidermal cell wall-bound lipids in *Arabidopsis* is unusual and strikingly similar to that of suberin in which long-chain α-,ω-dicarboxylic FAs generally constitute about 30–35% of its aliphatic domain (Franke et al. 2005). Suberin is an insoluble polymeric material that is directly attached to cell walls of specialized cells, e.g., endodermis and epidermis of the root, and involved in cell wall cross-linking (Kolattukudy 2001c). In this context, in addition to being essential cutin components, long-chain α-,ω-dicarboxylic FAs may play an indispensable general role in the cross-linking of the epidermal cell wall in *Arabidopsis* (Yephremov and Schreiber 2005). This role may be less significant in other species where the progressive cuticle thickening due to increasingly massive deposition of ω-hydroxy FA polyesters could not only make detection of dicarboxylates more difficult (Bonaventure et al. 2004) but also compensate for their deficiency.

With regard to the cuticular mutant phenotype, according to the above scenario, without proper strengthening by lipid molecules, the outermost portion of the primary cell wall in *hth-12* is not able to form the rigid boundary that normally prevents the cell-wall material from being pushed outward. Repeating this process probably results in multilayered deposits of electron-opaque cuticular polymers intervening in the electron-translucent material of the cell wall.

The occurrence of the stiff cross-linking of the epidermal cell wall is supported by the observation that in the *ad1* mutant of maize, sutures formed through direct contact between epidermal cell walls like in *hth-12*—without involvement of the cuticle—are resistant to cell-wall-degrading enzymes (Sinha and Lynch 1998). Interestingly, the fusion sutures in *lcr* also do not show deposition of darkly staining material that delineates the cuticle proper (Wellesen et al. 2001), while an electron-dense material accumulates between the cell walls of the adherent epidermal cells in *fdh* (Lolle et al. 1992). The reason for this difference is unclear; one possibility is that this may reflect accumulation of certain FAs or other compounds in cuticular polyesters of these mutants.

In contrast to cutin, suberin is rich in aromatic compounds (Kolattukudy 2001c). Although, the presence of an aromatic domain normally associated with

lignin and suberin deposition has been detected in the epidermal subcuticular cell walls, e.g., of growing tomato fruit but not in the cuticle (Andrews et al. 2002), virtually nothing is known about the aliphatic composition of the subcuticular cell walls. Similarly, the outer epidermal cell walls in *Arabidopsis* roots show the autofluorescence (Franke et al. 2005), which is ascribed to aromatics; however, their aliphatic composition is not known. It remains to be seen, therefore, if the postulated cross-linking process may be identical to suberization or represents another way of strengthening of the cellulose polymers that requires the use of α-,ω-dicarboxylic FAs. The occurrence of *ACE/HTH* (Fig. 4g, h) as well as other cuticular genes (Yephremov and Schreiber 2005; A. Yephremov, unpublished data) in root epidermal cells, which do not form a protective polyester membrane on the exterior surface that is detectable by TEM and histochemical staining for suberin, supports the latter model and suggests a general role for α-,ω-dicarboxylic FAs in the formation of the outer epidermal cell wall in plants.

Contribution of 2-hydroxy FAs to leaf residual-bound lipids in *Arabidopsis*

Our results show that, in addition to the presence of high proportion of α-,ω-dicarboxylic FAs, the composition of leaf residual-bound lipids in *Arabidopsis* is characterized by a significant amount, 38%, of saturated 2-hydroxy FAs ranging from C16 to C28 with 2-hydroxy-tetracosanoic and 2-hydroxy-tetracosenoic acids as major components (Table 1).

2-Hydroxy FAs are constituents of eukaryotic plasma membrane sphingolipids. They are also one of five prominent aliphatic classes in suberin in plants (Schreiber et al. 1999); however, the molecular details of their biosynthesis are largely unknown.

Although the recent compositional analysis of residual-bound lipids in *Arabidopsis*, including epidermal peels (Bonaventure et al. 2004), did not report the presence of 2-hydroxylates, we are confident that contamination of the leaf residual-bound lipids by plasma membrane lipids was minimal in our samples for the following reason. After an extensive extraction with organic solvents, no traces of the highly unsaturated FAs 16:3 and 18:3 that account for 70% of all the FAs in *Arabidopsis* leaf tissue (Branen et al. 2001) have been detected in our leaf samples, while prominent peaks for 2-hydroxy FAs were observed as indicated in the chromatogram (Fig. 3c). It is unclear which methodological differences between the two sets of data (e.g., hydrolysis conditions, chromatographic separation conditions) can account for the observed discrepancy. The data presented in this paper do not indicate whether 2-hydroxylates are components of any cuticular lipids in the epidermis, or that they are associated with underlying tissues, e.g., vascular bundles, or both. However, 2-hydroxy FAs were detected in *Arabidopsis* cutin and suberin isolated with the use of polysaccharide hydrolases (Franke et al. 2005).

Does *ACE/HTH* function cell autonomously?

Examination of somatic reversions in petals suggests *ACE/HTH* acts cell autonomously in controlling cell morphology in the epidermis. Considering the central role that the cell wall plays in morphogenesis, it is possible that the changes in organ and cell morphology in the specific class of epidermal mutants, e.g., *fdh* and *lcr*, indicate their inability to strengthen the cuticular membrane or cuticular layer of the primary cell wall. These results are consistent with ACE/HTH being directly or indirectly involved in biosynthesis of leaf C16 and C18 polyester monomers required for the formation of the outer epidermal cell wall.

However, a recent report which noted genome-wide reversing of sequence changes in DNA in EMS-induced *hth* alleles (Lolle et al. 2005) may support the idea that *HTH* acts non-cell autonomously. For mutations to be transmitted to succeeding generations, the reversing events have to occur within the subepidermal L2 layer, which gives rise to gametes, but our results demonstrate that *ACE/HTH* expression is restricted to the epidermal L1 layer, showing specific non-cell autonomous activity of the *hth* mutation in this process.

Does *Arabidopsis* show a way to improve cuticle in crop plants?

The cuticle membrane in *Arabidopsis*—a weed native to a relatively humid climate of Europe—is fragile and only 20–80 nm thick while in many other plants it is in the range of some micrometers (Nawrath 2002). How does the epidermis, covered with such a thin membrane, manage to withstand natural stresses and pathogens? The results accumulated to date raise an interesting question whether the α-,ω-dicarboxylic FA-based cuticular covering in *Arabidopsis* has superior mechanical and protective properties compared to ω-hydroxy FA-based covering in co-inhabitant plants. If so, then it offers the possibility of improving, e.g., drought resistance in cultivated plants, by increasing the proportion of α-,ω-dicarboxylic FAs in cuticular polyesters.

References

Aharoni A, Dixit S, Jetter R, Thoenes E, van Arkel G, Pereira A (2004) The SHINE clade of AP2 domain transcription factors activates wax biosynthesis, alters cuticle properties, and confers drought tolerance when overexpressed in *Arabidopsis*. Plant Cell 16:2463–2480

Agrawal VP, Kolattukudy PE (1977) Biochemistry of suberization: ω-hydroxyacid oxidation in enzyme preparations from suberizing potato tuber disks. Plant Physiol 59:667–672

Andrews J, Adams SR, Burton KS, Evered EC (2002) Subcellular localization of peroxidase in tomato fruit skin and the possible implications for the regulation of fruit growth. J Exp Bot 53:2175–2191

Araki T, Nakatani-Goto M (1999) *Arabidopsis* ADHESION OF CALYX EDGES (ACE), genomic. Published only in DataBase

Baud S, Bellec Y, Miquel M, Bellini C, Caboche M, Lepiniec L, Faure J-D, Rochat C (2004) *gurke* and *pasticcino3* mutants affected in embryo development are impaired in acetyl-CoA carboxylase. EMBO Rep 5:515–520

Bellec Y, Harrar Y, Butaeye C, Darnet S, Bellini C, Faure J-D (2002) PASTICCINO2 is a protein tyrosine phosphatase-like involved in cell proliferation and differentiation in *Arabidopsis*. Plant J 32:713–722

Bonaventure G, Beisson F, Ohlrogge J, Pollard M (2004) Analysis of the aliphatic monomer composition of polyesters associated with *Arabidopsis* epidermis: occurrence of octadeca-*cis*-6, *cis*-9-diene-1,18-dioate as the major component. Plant J 40:920–930

Branen JK, Chiou T-J, Engeseth NJ (2001) Overexpression of acyl carrier protein-1 alters fatty acid composition of leaf tissue in *Arabidopsis*. Plant Physiol 127:222–229

Broun P, Poindexter P, Osborne E, Jiang C-Z, Riechmann JL (2004) WIN1, a transcriptional activator of epidermal wax accumulation in *Arabidopsis*. Proc Natl Acad Sci USA 101:4706–4711

Browse J, McCourt PJ, Somerville CR (1986) Fatty acid composition of leaf lipids determined after combined digestion and fatty acid methyl ester formation from fresh tissue. Anal Biochem 152:141–145

Chen X, Goodwin SM, Boroff VL, Liu X, Jenks MA (2003) Cloning and characterization of the *WAX2* gene of *Arabidopsis* involved in cuticle membrane and wax production. Plant Cell 15:1170–1185

Cheng Q, Liu H-T, Bombelli P, Smith A, Slabas AR (2004) Functional identification of AtFao3, a membrane bound long chain alcohol oxidase in *Arabidopsis thaliana*. FEBS Lett 574:62–68

Dreveny I, Gruber K, Glieder A, Thompson A, Kratky C (2001) The hydroxynitrile lyase from almond: a lyase that looks like an oxidoreductase. Structure 9:803–815

Efremova N, Schreiber L, Bär S, Heidmann I, Huijser P, Wellesen K, Schwarz-Sommer Z, Saedler H, Yephremov A (2004) Functional conservation and maintenance of expression pattern of *FIDDLEHEAD*-like genes in *Arabidopsis* and *Antirrhinum*. Plant Mol Biol 56:821–837

Franke R, Briesen I, Wojciechowski T, Faust A, Yephremov A, Nawrath C, Schreiber L (2005) Apoplastic polyesters in *Arabidopsis* surface tissues—a typical suberin and a particular cutin. Phytochemistry 66:2643–2658

Haberer G, Erschadi S, Torres-Ruiz RA (2002) The *Arabidopsis* gene *PEPINO/PASTICCINO2* is required for proliferation control of meristematic and non-meristematic cells and encodes a putative anti-phosphatase. Dev Genes Evol 212:542–550

Holmquist B, Vallee BL (1991) Human liver class III alcohol and glutathione dependent formaldehyde dehydrogenase are the same enzyme. Biochem Biophys Res Commun 178:1371–1377

Kolattukudy PE (2001a) Cutin from plants. In: Doi Y, Steinbuechel A (eds) Biopolymers: polyesters I—biological systems and biotechnological production, vol. 3a. Wiley, Muenster, Germany, pp. 1–35

Kolattukudy PE (2001b) Polyesters in higher plants. In: Babel W, Steinbuechel A (eds) Advances in biochemical engineering biotechnology. Biopolyesters, vol. 71. Springer, Berlin Heidelberg New York, pp. 1–49

Kolattukudy PE (2001c) Suberin from plants. In: Doi Y, Steinbuechel A (eds) Biopolymers: polyesters I—biological systems and biotechnological production, vol. 3a. Wiley, Muenster, Germany, pp. 41–68

Krolikowski KA, Victor JL, Wagler TN, Lolle SJ, Pruitt RE (2003) Isolation and characterization of the *Arabidopsis* organ fusion gene *HOTHEAD*. Plant J 35:501–511

Kurata T, Kawabata-Awai C, Sakuradani E, Shimizu S, Okada K, Wada T (2003) The *YORE–YORE* gene regulates multiple aspects of epidermal cell differentiation in *Arabidopsis*. Plant J 36:55–66

Le Bouquin R, Skrabs M, Kahn R, Benveniste I, Salaün JP, Schreiber L, Durst F, Pinot F (2001) CYP94A5, a new cytochrome P450 from *Nicotiana tabacum* is able to catalyze the oxidation of fatty acids to the ω-alcohol and to the corresponding diacid. Eur J Biochem 268:3083–3090

Lolle SJ, Cheung AY, Sussex IM (1992) *Fiddlehead*: an *Arabidopsis* mutant constitutively expressing an organ fusion program that involves interactions between epidermal cells. Dev Biol 152:383–392

Lolle SJ, Hsu W, Pruitt RE (1998) Genetic analysis of organ fusion in *Arabidopsis thaliana*. Genetics 149:607–619

Lolle SJ, Victor JL, Young JM, Pruitt RE (2005) Genome-wide non-mendelian inheritance of extra-genomic information in *Arabidopsis*. Nature 434:505–509

Nawrath C (2002) The biopolymers cutin and suberin. In: Somerville C, Meyerowitz E (eds) The *Arabidopsis* book. American Society of Plant Biologists, Rockville

Pruitt RE, Vielle-Calzada JP, Ploense SE, Grossniklaus U, Lolle SJ (2000) *FIDDLEHEAD*, a gene required to suppress epidermal cell interactions in *Arabidopsis*, encodes a putative lipid biosynthetic enzyme. Proc Natl Acad Sci USA 97:1311–1316

Schnurr J, Shockey J, Browse J (2004) The Acyl-CoA synthetase encoded by *LACS2* is essential for normal cuticle development in *Arabidopsis*. Plant Cell 16:629–642

Schreiber L, Hartmann K, Skrabs M, Zeier J (1999) Apoplastic barriers in roots: chemical composition of endodermal and hypodermal cell walls. J Exp Bot 50:1267–1280

Sieber P, Schorderet M, Ryser U, Buchala A, Kolattukudy PE, Métraux J-P, Nawrath C (2000) Transgenic *Arabidopsis* plants expressing a fungal cutinase show alterations in the structure and properties of the cuticle and postgenital organ fusions. Plant Cell 12:721–737

Sinha N, Lynch M (1998) Fused organs in the *adherent 1* mutation in maize show altered epidermal walls with no perturbations in tissue identities. Planta 206:184–195

Sorensen A-M, Krober S, Unte US, Huijser P, Dekker K, Saedler H (2003) The *Arabidopsis ABORTED MICROSPORES* (*AMS*) gene encodes a MYC class transcription factor. Plant J 33:413–423

Steiner-Lange S, Gremse M, Kuckenberg M, Nissing E, Schaechtele D, Spenrath N, Wolff M, Saedler H, Dekker K (2001) Efficient identification of *Arabidopsis* knock-out mutants using DNA-arrays of transposon flanking sequences. Plant Biol 3:391–397

Tanaka H, Onouchi H, Kondo M, Hara-Nishimura I, Nishimura M, Machida C, Machida Y (2001) A subtilisin-like serine protease is required for epidermal surface formation in *Arabidopsis* embryos and juvenile plants. Development 128:4681–4689

Tanaka H, Watanabe M, Watanabe D, Tanaka T, Machida C, Machida Y (2002) ACR4, a putative receptor kinase gene of *Arabidopsis thaliana*, that is expressed in the outer cell layers of embryos and plants, is involved in proper embryogenesis. Plant Cell Physiol 43:419–428

Tanaka T, Tanaka H, Machida C, Watanabe M, Machida Y (2004) A new method for rapid visualization of defects in leaf cuticle reveals five intrinsic patterns of surface defects in *Arabidopsis*. Plant J 37:139–146

Vanhanen S, West M, Kroon JTM, Lindner Nl, Casey J, Cheng Q, Elborough KM, Slabas AR (2000) A consensus sequence for long-chain fatty-acid alcohol oxidases from *Candida* identifies a family of genes involved in lipid omega-oxidation in yeast with homologues in plants and bacteria. J Biol Chem 275:4445–4452

Watanabe M, Tanaka H, Watanabe D, Machida C, Machida Y (2004) The ACR4 receptor-like kinase is required for surface formation of epidermis-related tissues in *Arabidopsis thaliana*. Plant J 39:298–308

Wellesen K, Durst F, Pinot F, Benveniste I, Nettesheim K, Wisman E, Steiner-Lange S, Saedler H, Yephremov A (2001) Functional analysis of the *LACERATA* gene of *Arabidopsis* provides evidence for different roles of fatty acid ω-hydroxylation in development. Proc Natl Acad Sci USA 98:9694–9699

Williamson RE, Burn JE, Hocart CH (2001) Cellulose synthesis: mutational analysis and genomic perspectives using *Arabidopsis thaliana*. Cell Mol Life Sci 58:1475–1490

Wisman E, Cardon GH, Fransz P, Saedler H (1998) The behaviour of the autonomous maize transposable element *En/Spm* in *Arabidopsis thaliana* allows efficient mutagenesis. Plant Mol Biol 37:989–999

Xiao F, Goodwin MS, Xiao Y, Sun Z, Baker D, Tang X, Jenks MA, Zhou J-M (2004) *Arabidopsis* CYP86A2 represses *Pseudomonas syringae* type III genes and is required for cuticle development. EMBO J 23:2903–2913

Yephremov A, Saedler H (2000) Display and isolation of transposon-flanking sequences starting from genomic DNA or RNA. Plant J 21:495–505

Yephremov A, Schreiber L (2005) The dark side of the cell wall: molecular genetics of plant cuticle. Plant Biosyst 139:74–79

Yephremov A, Wisman E, Huijser P, Huijser C, Wellesen K, Saedler H (1999) Characterization of the *FIDDLEHEAD* gene reveals a link between adhesion response and cell differentiation in the epidermis. Plant Cell 11:2187–2201

Yephremov A, Faust A, Kurdyukov S, Trenkamp S, Nawrath C, Franke R, Wojciechowski T, Efremova N, Voisin D, Toro F, Tietjen K, Schreiber L, Saedler H (2004) Safeguarding the cuticular wall. In: Xth cell wall meeting, Sorrento, 29 August–3 September 2004, Italy, p. 99